

UNIVERSITY OF BIRMINGHAM

Research at Birmingham

Probing cortical excitability using rapid frequency tagging

Zhigalov, Alexander; Herring, J.D.; Herpers, J.; Bergmann, T.O.; Jensen, Ole

DOI:

[10.1016/j.neuroimage.2019.03.056](https://doi.org/10.1016/j.neuroimage.2019.03.056)

License:

Creative Commons: Attribution (CC BY)

Document Version

Peer reviewed version

Citation for published version (Harvard):

Zhigalov, A, Herring, JD, Herpers, J, Bergmann, TO & Jensen, O 2019, 'Probing cortical excitability using rapid frequency tagging' *NeuroImage*. <https://doi.org/10.1016/j.neuroimage.2019.03.056>

[Link to publication on Research at Birmingham portal](#)

Publisher Rights Statement:

Checked for eligibility: 02/04/2019
<https://doi.org/10.1016/j.neuroimage.2019.03.056>

General rights

Unless a licence is specified above, all rights (including copyright and moral rights) in this document are retained by the authors and/or the copyright holders. The express permission of the copyright holder must be obtained for any use of this material other than for purposes permitted by law.

- Users may freely distribute the URL that is used to identify this publication.
- Users may download and/or print one copy of the publication from the University of Birmingham research portal for the purpose of private study or non-commercial research.
- User may use extracts from the document in line with the concept of 'fair dealing' under the Copyright, Designs and Patents Act 1988 (?)
- Users may not further distribute the material nor use it for the purposes of commercial gain.

Where a licence is displayed above, please note the terms and conditions of the licence govern your use of this document.

When citing, please reference the published version.

Take down policy

While the University of Birmingham exercises care and attention in making items available there are rare occasions when an item has been uploaded in error or has been deemed to be commercially or otherwise sensitive.

If you believe that this is the case for this document, please contact UBIRA@lists.bham.ac.uk providing details and we will remove access to the work immediately and investigate.

Accepted Manuscript

Probing cortical excitability using rapid frequency tagging

A. Zhigalov, J.D. Herring, J. Herpers, T.O. Bergmann, O. Jensen

PII: S1053-8119(19)30256-3

DOI: <https://doi.org/10.1016/j.neuroimage.2019.03.056>

Reference: YNIMG 15732

To appear in: *NeuroImage*

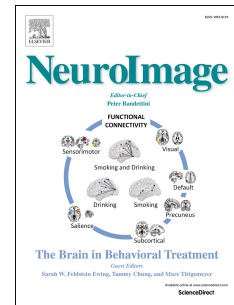
Received Date: 17 December 2018

Revised Date: 25 March 2019

Accepted Date: 25 March 2019

Please cite this article as: Zhigalov, A., Herring, J.D., Herpers, J., Bergmann, T.O., Jensen, O., Probing cortical excitability using rapid frequency tagging, *NeuroImage* (2019), doi: <https://doi.org/10.1016/j.neuroimage.2019.03.056>.

This is a PDF file of an unedited manuscript that has been accepted for publication. As a service to our customers we are providing this early version of the manuscript. The manuscript will undergo copyediting, typesetting, and review of the resulting proof before it is published in its final form. Please note that during the production process errors may be discovered which could affect the content, and all legal disclaimers that apply to the journal pertain.



Probing cortical excitability using rapid frequency tagging

Zhigalov, A.^{1*}, Herring, J.D.^{2*}, Herpers, J.³, Bergmann, T.O.^{2,4,5,6}, Jensen, O¹.

¹Centre for Human Brain Health, School of Psychology, University of Birmingham, UK

²Donders Institute, Radboud University Nijmegen, Nijmegen, The Netherlands

³Laboratory for Neurophysiology and Psychophysiology, KU Leuven, Leuven, Belgium

⁴Department of Neurology and Stroke, and Hertie Institute for Clinical Brain Research, University of Tübingen, Tübingen, Germany

⁵Institute of Medical Psychology and Behavioral Neurobiology, University of Tübingen, Tübingen, Germany

⁶Deutsches Resilienz Zentrum (DRZ), Johannes Gutenberg University Medical Center, Mainz, Germany

*A.Z and H.J.D contributed equally to this work.

Abstract

Frequency tagging has been widely used to study the role of visual selective attention. Presenting a visual stimulus flickering at a specific frequency generates so-called steady-state visually evoked responses. However, frequency tagging is mostly done at lower frequencies (<30 Hz). This produces a visible flicker, potentially interfering with both perception and neuronal oscillations in the theta, alpha and beta band. To overcome these problems, we used a newly developed projector with a 1440 Hz refresh rate allowing for frequency tagging at higher frequencies. We asked participants to perform a cued spatial attention task in which imperative pictorial stimuli were presented at 63 Hz or 78 Hz while measuring whole-head magnetoencephalography (MEG). We found posterior sensors to show a strong response at the tagged frequency. Importantly, this response was enhanced by spatial attention. Furthermore, we reproduced the typical modulations of alpha band oscillations, i.e., decrease in the alpha power contralateral to the attentional cue. The decrease in alpha power and increase in frequency tagged signal with attention correlated over subjects. We hereby provide proof-of-principle for the use of high-frequency tagging to study sensory processing and neuronal excitability associated with attention.

Introduction

Frequency tagging has been successfully used to study selective stimulus processing in EEG studies (e.g., (Müller et al., 2006, 2003, 1998; Norcia et al., 2015; Vialatte et al., 2010)). The technique has also been applied in MEG studies to investigate visual perception (Parkkonen et al., 2008) as well as the engagement of representational selective areas in the ventral stream (Baldauf and Desimone, 2014). With frequency tagging, a stimulus (usually visual or auditory) is presented at a fixed frequency, which then produces robust steady-state visually evoked potentials or fields (respectively SSVEPs or SSVEFs for EEG and MEG), resulting in

37 a power increase at the tagged frequency (Vialatte et al., 2010). These responses are for
38 instance enhanced by attention (Morgan et al., 1996; Müller et al., 2006) and reflect
39 subjective perception in a bi-stable perception task (Parkkonen et al., 2008). As such they are
40 a useful tool for investigating mechanisms of attention and perception in humans. Typically,
41 frequency tagging is applied at lower frequencies (<30 Hz), which is associated with flicker
42 perception and may interfere with task performance. It also creates a problem when relating
43 frequency tagging to neuronal oscillations in e.g. the alpha (8 – 13 Hz) and beta band (15 –
44 30 Hz) since frequency tagging is likely to entrain or interfere with spontaneous neuronal
45 oscillations as well (Keitel et al., 2014; Spaak et al., 2014). In this study, we use a newly
46 developed projector that allows us to perform frequency tagging at higher frequencies and
47 hence to investigate neuronal excitability and visual attention in relation to endogenous
48 oscillations in the alpha band.

49 Neuronal oscillations have been shown to play a key role in the processing of sensory
50 information by synchronizing neuronal firing and modulating synaptic input (Schroeder and
51 Lakatos, 2009). For example, alpha oscillations have been hypothesized to support active
52 inhibition of brain regions processing task-irrelevant, and possibly distracting, stimuli (Foxe
53 and Snyder, 2011; Jensen and Mazaheri, 2010; Klimesch et al., 2007). This is underscored by
54 the findings that posterior alpha oscillations are strongly modulated by spatial attention
55 (Händel et al., 2011; Thut et al., 2006; Worden et al., 2000). Additionally, the phase of alpha
56 has been shown to modulate perception (Mathewson et al., 2011; Vanrullen et al., 2011) and
57 cortical excitability (Dugué et al., 2011; Scheeringa et al., 2011; Spaak et al., 2012).

58 In this study, we apply frequency tagging between 60 and 80 Hz in order to probe neocortical
59 excitability in relation to alpha oscillations. A previous study by Christoph Herrmann
60 (Herrmann, 2001) has shown that rapidly flickering LED can drive the visual cortex as
61 measured by human EEG up to around 100 Hz. Intracranial recordings in monkeys and
62 humans have demonstrated that neuronal spiking in visual regions is entrained by the refresh
63 rate of a CRT computer monitor (60 Hz) (Krolak-Salmon et al., 2003; Sandström et al., 1997;
64 Williams et al., 2004). We applied frequency tagging above 60 Hz using a projector with a
65 1440 Hz refresh rate while recording whole-head MEG. This was done while subjects
66 attended to flickering face and house stimuli in a cued spatial attention paradigm. The aim
67 was to determine if cortical excitability as modulated by spatial attention could be estimated
68 using rapid frequency tagging. Our core assumption is that the amplitude of MEG signal at
69 the tagged frequency reflects neuronal excitability. Furthermore, we expect neuronal
70 excitability to increase with spatial attention and thus the tagged signal as well. A second aim
71 was to investigate the relationship between alpha band oscillations and the cortical
72 excitability assessed by rapid frequency tagging.

73 **Materials and Methods**

74 *Participants*

75 Participants were recruited from a participant database of the Radboud University Nijmegen.
76 Twenty-five healthy (17 females, aged 26 ± 10 (mean \pm SD)) participants partook in the

77 study. Two of the subjects were excluded due to an excessive amount of rejected trials.
78 Written informed-consent was acquired before enrolment in the study. All subjects
79 conformed to standard inclusion criteria for MEG experiments. Subjects had normal or
80 corrected-to-normal vision. The study was approved by the local ethics committee (CMO
81 region Arnhem/Nijmegen). Subjects received financial compensation of 8 euros per hour or
82 were compensated in course credits.

83 *Attention Task*

84 Participants performed a spatial attention task (4 blocks of 15 minutes) in which they had to
85 allocate attention to either the left, or the right visual hemifield, depending on a cue presented
86 at the start of each trial (Fig. 1).

87 -----
88 **Figure 1 about here**
89 -----

90 Each trial started with a fixation cross (500 ms) followed by an arrow (150 ms) indicating the
91 hemifield that the participants had to attend to (attentional cue), while fixating on the center
92 of the screen. The fixation cross was shown for 350 ms after the attentional cue, and then
93 stimuli were presented in the left and right visual hemifield for 1500 ms. Participants were
94 instructed to detect a vertical flip of the attended stimulus. Flips occurred at the end of trial in
95 25% of trials. In 20% of these trials, the flip was on the cued side, while in 5% of the trials
96 (catch trials), the flip was in the hemifield opposite to the cued side, and participants had not
97 to respond. Participants responded to the vertical flip by button presses with either index
98 finger (flip on the left) or middle finger (flip of the right). The duration of the flipped
99 stimulus was adjusted using QUEST adaptive staircase procedure (Watson and Pelli, 1983) to
100 attain 80% correct responses. The initial duration of the flipped stimuli was 10 ms and it
101 varied between 2 and 30 ms during the session controlled by the QUEST procedure. The
102 validity of the responses was indicated on the screen as correct ("CORRECT"), incorrect
103 ("INCORRECT"), or missed ("MISS") response. Next trial began following a random
104 interval of 500 ± 250 ms. Such relatively short inter-stimulus interval may influence the
105 neuronal responses in the subsequent trials; however, the random stimulus onset reduces this
106 effect. The experimental paradigm was implemented in MATLAB 2017b (Mathworks Inc.,
107 Natick, USA) using Psychophysics Toolbox 3.0.11 (Kleiner et al., 2007).

108 *Visual stimuli*

109 Pairs of stimuli (face and house) were presented simultaneously in the lower left and right
110 visual field (8.3 degrees eccentricity). Different combinations of faces and houses
111 (comprising ten faces and ten houses) were presented in random order over the trials.
112 Luminance of the grayscale stimuli was normalized using the SHINE Toolbox for MATLAB
113 (Willenbockel et al., 2010) and a circular mask was applied to the images (see, Fig. 1).
114 Stimuli were presented at a rate of respectively 63 Hz and 78 Hz (counter-balanced over
115 trials). The presentation rate was achieved by modulating transparency of the stimulus with a

116 sinusoid at the target frequency, phase-locked across trials. Direction of attention, pairing of
117 face-house stimuli and tagging frequencies were counterbalanced over trials.

118 *Projector*

119 To achieve a high rate of stimuli presentation, we used a GeForce GTX960 2GB graphics
120 card in combination with a PROPixx DLP LED projector (VPixx Technologies Inc., Saint-
121 Bruno-de-Montarville, Canada). This projector provides a refresh rate up to 1440 Hz by
122 dividing each frame received from the graphics card (at 120 Hz) into multiple frames.
123 Basically, the projector divides each received frame (1920 x 1200 pixels) into four equally
124 sized quadrants (960 x 600 pixels), allowing for a fourfold increase in refresh rate (480 Hz).
125 Colour (RGB) images presented in each quadrant can be further converted to a grayscale
126 representation by equalizing all components of RGB code. As such, this allows for an
127 increased refresh rate of 120 Hz by a factor of 4 times 3 (1440 Hz) when presenting grayscale
128 images with a resolution of 960 x 600 pixels.

129 *MRI data acquisition*

130 A high-resolution T1-weighted image (TR = 2300 ms, TE = 3.03 ms, TI = 1100 ms, 1.0 mm³
131 isotropic resolution, 192 sagittal slices) was acquired using a 3T MAGNETOM Skyra
132 (Siemens Healthcare, Erlangen, Germany).

133 *MEG data acquisition*

134 MEG was acquired using a 275-sensor axial gradiometer CTF system (CTF MEG systems,
135 Coquitlam, Canada). The MEG data was low-pass filtered at 300 Hz using embedded anti-
136 aliasing filters and sampled at 1200 Hz. Head position of the participants was continuously
137 monitored throughout the experiment using three head-localization coils placed on the nasion
138 and both periauricular points (Stolk et al., 2013).

139 *MEG data preprocessing*

140 MEG data were analysed using MATLAB and the Fieldtrip toolbox (Oostenveld et al., 2011).
141 The data were segmented into 3.5 s epochs; -1.5 to 2 s relative to the onset of flickering
142 stimulation. The data were further down-sampled to 300 Hz and ICA unmixing matrices were
143 calculated using the 'infomax' algorithm (Makeig et al., 1996) on the first 90 principal
144 components of the data. Components containing topographies and time courses clearly
145 matching cardiobalistic activity and eye-blinks were rejected from the data. The trials
146 containing large amplitude events (above 5 SD) were rejected. The number of such trials has
147 not exceeded of 5% of total amount of trials.

148 *Sensor-level analysis*

149 Synthetic planar gradients were calculated to ease interpretation of the topography of power
150 measurements (Bastiaansen and Knösche, 2000). The planar gradient power was combined
151 by summing the orthogonal components for each sensor location.

152 To estimate the effect of attention on power at the tagging frequencies or neuronal
 153 oscillations, the attention modulation index (AMI) was calculated. To this end, spectral
 154 power for time-frequency representations (TFR) was computed using Fourier transform (FT)
 155 for each sensor and epoch from -1.5 to 2 s relatively to stimulus onset. The spectral power
 156 was computed for multiple moving-time windows (1 s length and 0.05 s step) weighted by
 157 the Hanning taper, and over a range of frequencies (1 – 100 Hz). The effect of spatial
 158 attention for the left sensors was calculated as follows:

$$159 \quad \text{AMI}_{\{SL\}} = (P_{AR\{SL\}} - P_{AL\{SL\}}) / (P_{AR\{SL\}} + P_{AL\{SL\}}) \quad (1)$$

160 where SL denotes the subset of left sensors (similarly, SR denotes the subset of right
 161 sensors); P_{AL} and P_{AR} denote spectral power averaged over trials “attention left” and
 162 “attention right”, respectively. The AMI for the right sensors was computed in the same
 163 manner, and the resulting AMI was obtained by combining AMI for the left and right sensors
 164 with inverse polarity as follows:

$$165 \quad \text{AMI} = \text{AMI}_{\{SL\}} - \text{AMI}_{\{SR\}} \quad (2)$$

166 In case of all sensors AMI (see, Figure 4), we computed the spatial patterns as follows:

$$167 \quad \text{AMI} = (P_{AR} - P_{AL}) / (P_{AR} + P_{AL}) \quad (3)$$

168 where P_{AL} and P_{AR} denote spectral power averaged over trials “attention left” and “attention
 169 right”, respectively.

170 *Statistical comparisons*

171 Unless specified otherwise, conditions were compared using two-sided paired-sample t-tests.
 172 To statistically quantify the AMI in spatial domain, we used cluster-based permutation
 173 statistics (Maris and Oostenveld, 2007), which allow controlling for multiple comparisons
 174 over sensors.

175 **Results**

176 Subjects performed a cued spatial attention task and were instructed to press a button if a
 177 stimulus flipped vertically on the cued side (left or right). In each trial, a pair of face/house
 178 stimuli appeared for 1.5 s in the left and right visual hemifield (Fig. 1). Each stimulus was
 179 flickering at either 63 Hz or 78 Hz. The location of the face and house stimulus (left or right
 180 hemifield), tagging frequency (63 or 78 Hz), and direction of attention were counterbalanced
 181 over trials throughout the experiment.

182 *Behaviour*

183 Behavioural results demonstrated that participants were able to detect flips in the attended
 184 hemifield while ignoring flips in the unattended hemifield. The average hit rate was $0.75 \pm$
 185 0.05 (mean \pm SD) and the average reaction time was 0.47 ± 0.03 s (mean \pm SD).

186 *Spatial attention modulates responses of frequency-tagged stimuli*

187 To assess the response in the early visual cortex to the flickering stimuli, we calculated time-
188 locked averages of the event-related fields pooling data over stimulus type (face, house) and
189 direction of attention (left, right). Visual stimulation at the tagging frequencies produced clear
190 steady-state visual evoked fields (SSVEFs) in occipital sensors (Fig. 2A,B). The SSVEFs
191 lasted for the entire stimulation period and were markedly larger for 63 Hz compared to 78
192 Hz, as evident by a significant main effect of tagging frequency.

193

Figure 2 about here

194

196 We calculated the power spectra for each trial and then averaged over the trials. The sensors
197 were selected according to the strongest response at the tagging frequencies for all the
198 participants (Fig. 2C). The group-level normalized power spectra showed pronounced peaks
199 in the tagging frequencies at the selected occipital sensors (Fig. 2D), suggesting that the
200 frequency tagging method produces reliable responses in majority of the participants.

201 To quantify the effect of attentional modulation of power at the tagging signals we calculated
202 the attention modulation index (AMI; see Materials and Methods). The AMI indicates the
203 power at sensors contralaterally to the attended hemifield minus the power ipsilaterally
204 (normalized by the sum); as such the figures reflect attention ‘ON’ minus attention ‘OFF’.
205 The AMI was computed for the entire trial interval from -1.5 to 2 s (relatively to stimulus
206 onset) using time-frequency representations of power (Fig. 3A). This was done for the
207 sensors shown in Fig. 2C. The signals at the tagged frequencies increased with attention; i.e.
208 they increased in the hemisphere contralateral to the attended hemifield. The alpha power was
209 relatively suppressed in the hemisphere contralateral to attention. The AMI was then
210 averaged over time bins in the 0.5 – 1.5 s interval to reduce the contribution of the initial
211 evoked response (Fig. 3B). The AMI was significantly different from zero ($t_{22} > 5.64$, $p <$
212 10^{-5} , uncorrected) in both the alpha band and at the tagging frequencies. However, AMI at 63
213 Hz was significantly larger than AMI at 78 Hz ($t_{22} = 2.74$, $p < 0.01$), suggesting that the
214 efficacy of the response decreases at high frequencies (above 20 Hz) as a function of
215 (tagging) frequency.

216 The AMI was derived as a difference in power between trials “attention left” and “attention
217 right” (see, equation 1), and hence, it does not indicate whether the difference is related to
218 ipsilateral increase or contralateral decrease in power at the alpha frequency (and opposite in
219 the tagging frequencies). To clarify this, we quantified the relative change in power compared
220 to the baseline as follows, $\Delta P = (P_{\text{stimulation}} - P_{\text{baseline}}) / P_{\text{baseline}}$, where P_{baseline} and $P_{\text{stimulation}}$
221 denote power at the baseline and stimulation, respectively. The power at the alpha
222 frequencies showed larger decrease contralaterally to stimulation side and the power at the
223 tagging frequencies showed an opposite change (Fig. 3C, D).

224

Figure 3 about here

225

226

227 Using cluster-based permutation test controlling for multiple comparisons over sensors (see
 228 Materials and Methods), we identified the clusters of sensors at which power was
 229 significantly modulated by attention (Fig. 4). The spatial clusters of AMI in the alpha band
 230 and the tagging frequencies were over occipito-parietal areas; however, the alpha frequency
 231 clusters were located more posterior compared to those of the tagging frequencies. We
 232 quantified the overlap between clusters using the Jaccard (or Intersection over Union) index.
 233 The results of such method should be taken with caution because the cluster size is strongly
 234 affected by the signal-to-noise ratio and by the metric of statistical testing. The spatial
 235 clusters at the alpha and higher tagging frequency showed a moderate (nearly 60%) overlap
 236 as indicated by the Jaccard index. The spatial map of AMI at the alpha frequency was well in
 237 line with previous observations (e.g., (Foxye and Snyder, 2011; Händel et al., 2011; Thut et
 238 al., 2006; van Ede et al., 2011; Worden et al., 2000)), suggesting that the spatial attention
 239 related modulations of alpha activity are preserved despite the frequency tagging. Clusters at
 240 the lower (63 Hz) and higher (78 Hz) tagging frequencies showed a strong (over 90%)
 241 overlap as indicated by the Jaccard index; however, the clusters at 63 Hz were slightly larger
 242 compared to those for the higher frequency (78 Hz).

243 -----
 244 **Figure 4 about here**
 245 -----

246 *Relationship between AMI at the alpha and tagging frequencies*

247 Considering the inverse relationship between the attentional modulation in the alpha band and
 248 the tagging frequencies (see Fig. 4), we tested whether participants with a stronger
 249 modulation of alpha power have stronger power modulation at the tagging frequencies. To
 250 this end, we derived the individual AMI of the alpha band and the tagging frequencies (63
 251 and 78 Hz combined) and assessed their correlation over subjects. We defined separate masks
 252 for the alpha and tagging frequencies (Fig. 5A) by selecting sensors expressing the 10% of
 253 largest absolute AMI values (see Fig. 4). We observed a robust correlation ($r = -0.47$, $p <$
 254 0.03 ; Spearman correlation) between individual AMIs (Fig. 5B). This suggests that
 255 participants demonstrating stronger alpha modulation had also stronger modulation at the
 256 tagging frequencies. Additionally, we assessed the Spearman correlation between the
 257 individual AMI of the alpha and each tagging frequency, separately. The correlation was
 258 significant for the lower tagging frequency (63 Hz; $r = -0.51$, $p < 0.01$), but it was not
 259 significant for the higher tagging frequency (78 Hz; $r = -0.24$, $p > 0.26$). This result could be
 260 partially explained by lower signal-to-noise ratio at the higher frequencies.

261 -----
 262 **Figure 5 about here**
 263 -----

264 To test whether the relationship between AMI at the alpha and tagging frequencies holds at
 265 the single trial level, we computed the lateralization index (LI) for each trial as follows,

$$266 \quad LI_{(i)} = (P_{(i)\{SR\}} - P_{(i)\{SL\}}) / (P_{(i)\{SR\}} + P_{(i)\{SL\}}), \quad (4)$$

267 where $P_{(i)}$ denotes power for trial (i), SL and SR denote indices of the left and right sensors,
268 respectively. In contrast to the equation (1), we subtracted left and right sensors instead of
269 “attention left” and “attention right” trials. The $LI_{(i)}$ were split into two categories “attention
270 left” and “attention right”, and correlation (and median split t-test) between LI at the alpha
271 and tagging frequencies was computed for each category separately. We did not find any
272 significant ($p > 0.05$) correlation (or median split t-statistics) between LI at the alpha and
273 tagging frequencies. A larger amount of trials is necessary to establish whether such a
274 relationship exists or not.

275

276 **Discussion**

277 We here demonstrate that tagging of visual stimuli at rapid frequencies (63 and 78 Hz) can
278 induce neuronal responses at the same frequencies in visual cortex. Spatial attention towards
279 a visual object produced stronger responses at the tagging frequency contralateral to the
280 direction of attention compared to the unattended stimulus. As such, the tagging signal
281 reflects the gain of neuronal excitability with spatial attention. Posterior alpha oscillations
282 decreased in magnitude in posterior regions contralateral compared to ipsilateral to the
283 direction of attention. This demonstrates that the alpha oscillations were not disrupted by the
284 tagging signal.

285 The correlation between individual modulations in the alpha and the power at the tagging
286 frequencies suggests a link between attentional mechanisms for the alpha power and tagging
287 frequencies. One possibility is that alpha modulated by attention determines the neuronal
288 excitability which then determines the increase in the frequency tagged responses. This
289 interpretation however only partially explains the correlation as the topographies of AMI at
290 the alpha and tagging frequencies did not perfectly overlap.

291 *Proof-of-principle: using rapid frequency-tagging to probe neocortical excitability*

292 This study provides proof-of-principle that rapid frequency tagging can be used to probe
293 brain mechanisms involved in processing of visual stimuli without affecting endogenous
294 oscillations in the alpha range. Previous studies have shown that it is possible to elicit
295 responses in early visual cortex by using flickering light emitting diodes (LED) at frequencies
296 up to 100 Hz (Herrmann, 2001). However, the use of discrete LEDs does not allow for
297 creating complex stimuli. In this study, we used a state-of-the-art LED projector that is
298 capable of presenting stimuli at a refresh rate of 1440 Hz. Thus, this projector allowed us to
299 modulate luminance of the stimulus at frequencies up to 720 Hz (the Nyquist frequency of
300 the projector). Similarly to the study of Herrmann (2001), we observed weaker neuronal
301 response for the stimuli tagged at 78 Hz compared to 63 Hz, although both stimuli were
302 modulated with the same intensity. This might be explained by the attenuation resulting from
303 the synaptic drives in the early visual stream. The time course of the post-synaptic potentials
304 are in the order of ~ 10 ms (Koch et al., 1996), which effectively creates a ~ 100 Hz low pass
305 filter. Another possibility is that the proximity of the frequency of the tagged signal to the
306 frequency of the individual gamma oscillations influences the magnitude of the tagged

307 response. These possibilities require further investigation in future studies where the tagging
308 over a broader frequency is systematically explored.

309 *Attention enhances neural response to tagging signal*

310 An assumption underlying the use of frequency tagging as a tool to study sensory processing
311 in the brain is that the EEG/MEG signal at the tagged frequency reflects underlying sensory
312 processing. We have shown here that spatial attention modulates power at the tagging
313 frequency in the expected direction; the response at the tagged frequency was enhanced when
314 attention was directed towards the stimulus and suppressed when attention was directed
315 away. This suggests that the gain increase associated with the allocation of spatial attention
316 results in increased neuronal excitation, which in turn is reflected by the power of the
317 frequency tagged MEG signal.

318 *Alpha oscillations are not disrupted by rapid frequency tagging*

319 The increase in neuronal response modulated by spatial attention has also been shown at the
320 lower (up to 30 Hz) tagging frequencies (e.g. (Müller et al., 2006; Toffanin et al., 2009)).
321 However, frequency tagging at lower frequencies (0.5–30 Hz) is likely to interfere with
322 endogenous neuronal oscillations. Most frequency tagging experiments are limited to
323 frequency bands below 30 Hz (e.g. (Müller et al., 2006; Norcia et al., 2015; Toffanin et al.,
324 2009)). In this case, the tagging signal produces visible a flicker and may potentially entrain
325 the ongoing oscillations (Spaak et al., 2014; Thut et al., 2011). This is especially evident
326 given that tagging produces the strongest neuronal response in the visual system at
327 frequencies between 12 Hz and 18 Hz (Kuś et al., 2013).

328 In our study, alpha oscillations in the posterior regions remained undisrupted by the rapid
329 frequency tagging. Alpha power increased ipsilaterally to the direction of attention and
330 decreased contralaterally as observed in numerous other studies (Händel et al., 2011; Thut et
331 al., 2006; Worden et al., 2000). Applying frequency tagging at higher frequencies therefore
332 makes is possible to in conjunction study the role of lower-frequency oscillations on sensory
333 processing.

334 In future work it would be interesting to investigate if the rapid frequency tagging entrains intrinsic
335 gamma oscillations or rather reflect a simple feedforward drive. Similar considerations have been put
336 forward for the alpha rhythm (Keitel et al., 2014). It would also be interesting to investigate the
337 relationship between the phase of the alpha oscillations and the frequency tagged signal. Indeed the
338 phase of alpha oscillations has been suggested to modulate perception rhythmically in a pulsed
339 inhibitory manner; and this modulation is dependent on attention (Kizuk and Mathewson, 2017). This
340 notion could be investigated in the context of a phase-code coordinated by the alpha rhythm as
341 proposed by Jensen and colleagues (Jensen et al., 2014).

342 *Does rapid frequency tagging entrain neuronal gamma oscillations?*

343 There are several studies (Adjamian et al., 2004; Murty et al., 2018; Muthukumaraswamy and
344 Singh, 2013) that attempted to apply stimulation at frequencies in the gamma range in order
345 to entrain endogenous gamma band oscillations (30–90 Hz). Such studies are important for

346 understanding the important function gamma band oscillations may have in neuronal
347 computations (Fries et al., 2007; Jensen et al., 2007; Varela et al., 2001). Bauer and
348 colleagues (Bauer et al., 2009) showed that attention could be captured by subliminally
349 perceived stimuli flickering at 50 Hz. Manipulating visual perceptual integration by
350 modulating the phase of externally driven gamma frequency stimulation has proven difficult
351 (Bauer et al., 2012). Future studies may explore to what extent the neuronal activity elicited
352 by rapid frequency tagging entrains endogenous gamma oscillations. If this is the case,
353 frequency tagging should be more efficient and result in a relative power increase when
354 applied at the frequency of the individual endogenous gamma oscillations. This could also be
355 investigated by pharmacological means. It is well established that GABAergic inhibition
356 from interneurons plays a crucial role for generating of gamma oscillations (Traub et al.,
357 1999). In support of this notion, we recently demonstrated that visual gamma oscillations in
358 humans increase when the GABAergic agonist Lorazepam is applied (Lozano-Soldevilla et al.,
359 2014). If rapid frequency-tagging entrains natural gamma oscillations, one would expect that
360 rapid-frequency tagging in the gamma band increases with the application of GABAergic
361 agonists.

362 **Conclusion**

363 We set out to investigate the feasibility of rapid frequency tagging to study the role of sensory
364 processing in the visual cortex. Our results show that it is indeed possible to measure
365 responses at the tagging frequencies and that these responses are modulated by spatial
366 attention. The modulation of alpha power was inversely related to the modulation in gamma
367 power. These findings provide important proof-of-principle that rapid frequency tagging can
368 be used to measure neuronal excitability of visual cortex in a stimulus specific manner to for
369 instance investigate spatial attention. Furthermore, the dynamical properties of the alpha band
370 oscillations were preserved despite the frequency tagging. Rapid frequency tagging is highly
371 advantageous to conventional frequency tagging at lower frequency (<20 Hz) as it does not
372 produce a visible flicker and furthermore the faster frequencies allow for investigating the
373 tagged response with a better temporal resolution. The stage is now set for applying
374 frequency tagging in combination with EEG or MEG to study the dynamical properties of the
375 visual system.

376 **Acknowledgements**

377

378 This work was supported by the James S. McDonnell Foundation Understanding Human
379 Cognition Collaborative Award (grant number 220020448) to O.J.; Wellcome Trust
380 Investigator Award in Science (grant number 207550) to O.J.; Royal Society Wolfson
381 Research Merit Award to O.J.

382

383 **Figure legends**

384 Fig. 1. Schematic representation of the experimental paradigm. After an attentional cue, a house-face
385 pair was presented at 63 and 78 Hz (counterbalanced over trials). In 20% of the trials, one of the

386 images was flipped vertically and required participant's response. In 5% of the trials (catch trials), the
 387 flip was in the hemifield opposite to the cued side and participants had to ignore this event.

388 Fig. 2. Event-related fields for a representative participant showed clear responses at the tagging
 389 frequencies. Note that the frequency tagged signals were presented with the same phase over trials.
 390 (A) Broadband (black line) and narrowband (red line) trial-averaged ERFs for 63 Hz stimulus
 391 (presented right) for the left occipital sensors (see panel C). (B) Trial-averaged ERFs for 78 Hz
 392 stimulus (presented right) for the left occipital sensors. (C) Left and right occipital MEG sensors that
 393 covered areas with the stronger power at the tagging frequencies for all the participants were used in
 394 the analysis. (D) Normalized group-level power spectra for the left sensors when the tagged image
 395 was presented at 63 Hz and 78 Hz in the right hemifield. Prior to computing individual power spectra,
 396 the trials were normalized by the standard deviation of time series over sensors. The line noise with
 397 peak near 50 Hz was cut out in the plot.

398 Fig. 3. Attention modulates power in the alpha band and at the tagging frequencies. (A) Time-
 399 frequency representation of the attention modulation index (AMI). The AMI reflects the power
 400 modulation in the sensors contra- versus ipsilateral to the attended hemifield for combined left and
 401 right occipital sensors (see Fig. 2C for sensors selection). The power was calculated per trial and then
 402 averaged. Black line indicates onset of the frequency tagged stimuli; the cue onset was at -0.5 s. (B)
 403 The AMI (averaged over time bins 0.5 – 1.5 s) at the group level. Dashed lines indicate *p*-values of
 404 the t-test comparing modulation index against zero (over participants). The effect is highly robust in
 405 the 8-12 Hz alpha band and at 63 and 78 Hz even if multiple comparisons over frequencies are
 406 considered. (C) Relative power change compared to the baseline (-1, -0.5 s) at the left sensors for
 407 trials "attention left" (cyan line; ipsilateral to the cue) and "attention right" (blue line; contralateral to
 408 the cue). (D) The same as (C) but for the right sensors for trials "attention right" (orange line;
 409 ipsilateral to the cue) and "attention left" (red line; contralateral to the cue).

410 Fig. 4. Group average topography maps of the AMI in the alpha band (10 ± 2 Hz) and tagging
 411 frequencies (63 and 78 Hz). Black dots indicate MEG sensors at which amplitude modulation index
 412 was significantly different from zero ($p < 0.05$, cluster-based permutation).

413 Fig. 5. Relationship between the modulation of alpha power and frequency tagging. (A)
 414 Spatial masks for the alpha and tagging frequencies. The masks were obtained by selecting
 415 sensors expression the 10% of largest absolute AMI values. (B) Scatter plot of individual
 416 AMI relating the alpha power modulation and the power combined for the tagging
 417 frequencies. Subjects with a strong alpha power modulation with attention were also subjects
 418 with a strong modulation of the tagged signals.

419

420 References

- 421 Adjamian, P., Holliday, I.E., Barnes, G.R., Hillebrand, A., Hadjipapas, A., Singh, K.D., 2004.
 422 Induced visual illusions and gamma oscillations in human primary visual cortex. *Eur. J.*
 423 *Neurosci.* 20, 587–592. <https://doi.org/10.1111/j.1460-9568.2004.03495.x>
- 424 Baldauf, D., Desimone, R., 2014. Neural Mechanisms of Object-Based Attention. *Science*
 425 (80-.). 344, 424–427. <https://doi.org/10.1126/science.1247003>
- 426 Bastiaansen, M.C., Knösche, T.R., 2000. Tangential derivative mapping of axial MEG

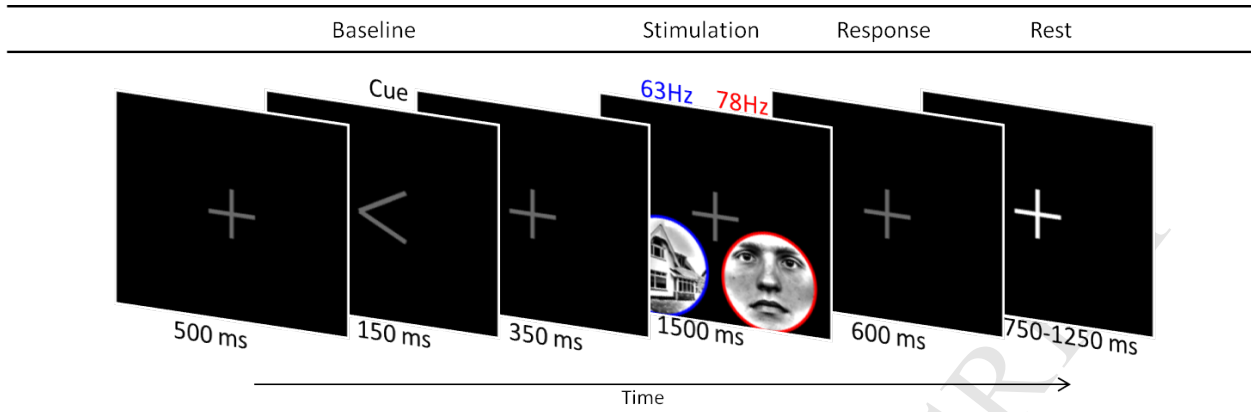
- 427 applied to event-related desynchronization research. *Clin. Neurophysiol.* 111, 1300–5.
- 428 Bauer, F., Cheadle, S.W., Parton, A., Müller, H.J., Usher, M., 2009. Gamma flicker triggers
429 attentional selection without awareness. *Proc. Natl. Acad. Sci. U. S. A.* 106, 1666–71.
430 <https://doi.org/10.1073/pnas.0810496106>
- 431 Bauer, M., Akam, T., Joseph, S., Freeman, E., Driver, J., 2012. Does visual flicker phase at
432 gamma frequency modulate neural signal propagation and stimulus selection? *J. Vis.* 12,
433 5–5. <https://doi.org/10.1167/12.4.5>
- 434 Dugué, L., Marque, P., VanRullen, R., 2011. The phase of ongoing oscillations mediates the
435 causal relation between brain excitation and visual perception. *J. Neurosci.* 31, 11889–
436 93. <https://doi.org/10.1523/JNEUROSCI.1161-11.2011>
- 437 Foxe, J.J., Snyder, A.C., 2011. The Role of Alpha-Band Brain Oscillations as a Sensory
438 Suppression Mechanism during Selective Attention. *Front. Psychol.* 2, 154.
439 <https://doi.org/10.3389/fpsyg.2011.00154>
- 440 Fries, P., Nikolić, D., Singer, W., 2007. The gamma cycle. *Trends Neurosci.* 30, 309–316.
441 <https://doi.org/10.1016/j.tins.2007.05.005>
- 442 Händel, B.F., Haarmeier, T., Jensen, O., 2011. Alpha oscillations correlate with the
443 successful inhibition of unattended stimuli. *J. Cogn. Neurosci.* 23, 2494–502.
444 <https://doi.org/10.1162/jocn.2010.21557>
- 445 Herrmann, C.S., 2001. Human EEG responses to 1-100 Hz flicker: resonance phenomena in
446 visual cortex and their potential correlation to cognitive phenomena. *Exp. brain Res.*
447 137, 346–53.
- 448 Jensen, O., Gips, B., Bergmann, T.O., Bonnefond, M., 2014. Temporal coding organized by
449 coupled alpha and gamma oscillations prioritize visual processing. *Trends Neurosci.* 37,
450 357–369. <https://doi.org/10.1016/j.tins.2014.04.001>
- 451 Jensen, O., Kaiser, J., Lachaux, J.-P., 2007. Human gamma-frequency oscillations associated
452 with attention and memory. *Trends Neurosci.* 30, 317–324.
453 <https://doi.org/10.1016/j.tins.2007.05.001>
- 454 Jensen, O., Mazaheri, A., 2010. Shaping functional architecture by oscillatory alpha activity:
455 gating by inhibition. *Front. Hum. Neurosci.* 4, 186.
456 <https://doi.org/10.3389/fnhum.2010.00186>
- 457 Keitel, C., Quigley, C., Ruhnau, P., 2014. Stimulus-Driven Brain Oscillations in the Alpha
458 Range: Entrainment of Intrinsic Rhythms or Frequency-Following Response? *J.*
459 *Neurosci.* 34, 10137–10140. <https://doi.org/10.1523/JNEUROSCI.1904-14.2014>
- 460 Kizuk, S.A.D., Mathewson, K.E., 2017. Power and Phase of Alpha Oscillations Reveal an
461 Interaction between Spatial and Temporal Visual Attention. *J. Cogn. Neurosci.* 29, 480–
462 494. https://doi.org/10.1162/jocn_a_01058
- 463 Kleiner, M., Brainard, D., Pelli, D., Ingling, A., Murray, R., Broussard, C., 2007. What's new
464 in psychtoolbox-3, Perception. [Pion Ltd.].
- 465 Klimesch, W., Sauseng, P., Hanslmayr, S., 2007. EEG alpha oscillations: The inhibition–
466 timing hypothesis. *Brain Res. Rev.* 53, 63–88.

- 467 <https://doi.org/10.1016/j.brainresrev.2006.06.003>
- 468 Koch, C., Rapp, M., Segev, I., 1996. A brief history of time (constants). *Cereb. Cortex* 6, 93–
469 101.
- 470 Krolak-Salmon, P., Hénaff, M.-A., Tallon-Baudry, C., Yvert, B., Guénot, M., Vighetto, A.,
471 Mauguière, F., Bertrand, O., 2003. Human lateral geniculate nucleus and visual cortex
472 respond to screen flicker. *Ann. Neurol.* 53, 73–80. <https://doi.org/10.1002/ana.10403>
- 473 Kuś, R., Duszyk, A., Milanowski, P., Łabęcki, M., Bierzyńska, M., Radzikowska, Z.,
474 Michalska, M., Zygierewicz, J., Suffczyński, P., Durka, P.J., 2013. On the quantification
475 of SSVEP frequency responses in human EEG in realistic BCI conditions. *PLoS One* 8,
476 e77536. <https://doi.org/10.1371/journal.pone.0077536>
- 477 Lozano-Soldevilla, D., ter Huurne, N., Cools, R., Jensen, O., 2014. GABAergic modulation
478 of visual gamma and alpha oscillations and its consequences for working memory
479 performance. *Curr. Biol.* 24, 2878–87. <https://doi.org/10.1016/j.cub.2014.10.017>
- 480 Makeig, S., Makeig, S., Bell, A.J., Jung, T., Sejnowski, T.J., 1996. Independent Component
481 Analysis of Electroencephalographic Data. *Adv. NEURAL Inf. Process. Syst.* 8, 145–
482 151.
- 483 Maris, E., Oostenveld, R., 2007. Nonparametric statistical testing of EEG- and MEG-data. *J.*
484 *Neurosci. Methods* 164, 177–90. <https://doi.org/10.1016/j.jneumeth.2007.03.024>
- 485 Mathewson, K.E., Lleras, A., Beck, D.M., Fabiani, M., Ro, T., Gratton, G., 2011. Pulsed out
486 of awareness: EEG alpha oscillations represent a pulsed-inhibition of ongoing cortical
487 processing. *Front. Psychol.* 2, 99. <https://doi.org/10.3389/fpsyg.2011.00099>
- 488 Morgan, S.T., Hansen, J.C., Hillyard, S.A., 1996. Selective attention to stimulus location
489 modulates the steady-state visual evoked potential. *Proc. Natl. Acad. Sci. U. S. A.* 93,
490 4770–4.
- 491 Müller, M.M., Andersen, S., Trujillo, N.J., Valdés-Sosa, P., Malinowski, P., Hillyard, S.A.,
492 2006. Feature-selective attention enhances color signals in early visual areas of the
493 human brain. *Proc. Natl. Acad. Sci. U. S. A.* 103, 14250–4.
494 <https://doi.org/10.1073/pnas.0606668103>
- 495 Müller, M.M., Malinowski, P., Gruber, T., Hillyard, S.A., 2003. Sustained division of the
496 attentional spotlight. *Nature* 424, 309–312. <https://doi.org/10.1038/nature01812>
- 497 Müller, M.M., Picton, T.W., Valdes-Sosa, P., Riera, J., Teder-Sälejärvi, W.A., Hillyard, S.A.,
498 1998. Effects of spatial selective attention on the steady-state visual evoked potential in
499 the 20-28 Hz range. *Brain Res. Cogn. Brain Res.* 6, 249–61.
- 500 Murty, D.V.P.S., Shirhatti, V., Ravishankar, P., Ray, S., 2018. Large Visual Stimuli Induce
501 Two Distinct Gamma Oscillations in Primate Visual Cortex. *J. Neurosci.* 38, 2730–
502 2744. <https://doi.org/10.1523/JNEUROSCI.2270-17.2017>
- 503 Muthukumaraswamy, S.D., Singh, K.D., 2013. Visual gamma oscillations: The effects of
504 stimulus type, visual field coverage and stimulus motion on MEG and EEG recordings.
505 *Neuroimage* 69, 223–230. <https://doi.org/10.1016/j.neuroimage.2012.12.038>
- 506 Norcia, A.M., Appelbaum, L.G., Ales, J.M., Cottareau, B.R., Rossion, B., 2015. The steady-

- 507 state visual evoked potential in vision research: A review. *J. Vis.* 15, 4.
508 <https://doi.org/10.1167/15.6.4>
- 509 Oostenveld, R., Fries, P., Maris, E., Schoffelen, J.-M., 2011. FieldTrip: Open source software
510 for advanced analysis of MEG, EEG, and invasive electrophysiological data. *Comput.*
511 *Intell. Neurosci.* 2011, 156869. <https://doi.org/10.1155/2011/156869>
- 512 Parkkonen, L., Andersson, J., Hämäläinen, M., Hari, R., 2008. Early visual brain areas reflect
513 the percept of an ambiguous scene. *Proc. Natl. Acad. Sci. U. S. A.* 105, 20500–4.
514 <https://doi.org/10.1073/pnas.0810966105>
- 515 Sandström, M., Lyskov, E., Berglund, A., Medvedev, S., Mild, K.H., 1997.
516 Neurophysiological effects of flickering light in patients with perceived electrical
517 hypersensitivity. *J. Occup. Environ. Med.* 39, 15–22.
- 518 Scheeringa, R., Mazaheri, A., Bojak, I., Norris, D.G., Kleinschmidt, A., 2011. Modulation of
519 visually evoked cortical fMRI responses by phase of ongoing occipital alpha
520 oscillations. *J. Neurosci.* 31, 3813–20. [https://doi.org/10.1523/JNEUROSCI.4697-](https://doi.org/10.1523/JNEUROSCI.4697-10.2011)
521 [10.2011](https://doi.org/10.1523/JNEUROSCI.4697-10.2011)
- 522 Schroeder, C.E., Lakatos, P., 2009. Low-frequency neuronal oscillations as instruments of
523 sensory selection. *Trends Neurosci.* 32, 9–18. <https://doi.org/10.1016/j.tins.2008.09.012>
- 524 Spaak, E., Bonnefond, M., Maier, A., Leopold, D.A., Jensen, O., 2012. Layer-specific
525 entrainment of γ -band neural activity by the α rhythm in monkey visual cortex. *Curr.*
526 *Biol.* 22, 2313–8. <https://doi.org/10.1016/j.cub.2012.10.020>
- 527 Spaak, E., de Lange, F.P., Jensen, O., 2014. Local entrainment of α oscillations by visual
528 stimuli causes cyclic modulation of perception. *J. Neurosci.* 34, 3536–44.
529 <https://doi.org/10.1523/JNEUROSCI.4385-13.2014>
- 530 Stolk, A., Todorovic, A., Schoffelen, J.-M., Oostenveld, R., 2013. Online and offline tools for
531 head movement compensation in MEG. *Neuroimage* 68, 39–48.
532 <https://doi.org/10.1016/j.neuroimage.2012.11.047>
- 533 Thut, G., Nietzel, A., Brandt, S.A., Pascual-Leone, A., 2006. Alpha-band
534 electroencephalographic activity over occipital cortex indexes visuospatial attention bias
535 and predicts visual target detection. *J. Neurosci.* 26, 9494–502.
536 <https://doi.org/10.1523/JNEUROSCI.0875-06.2006>
- 537 Thut, G., Schyns, P.G., Gross, J., 2011. Entrainment of perceptually relevant brain
538 oscillations by non-invasive rhythmic stimulation of the human brain. *Front. Psychol.* 2,
539 170. <https://doi.org/10.3389/fpsyg.2011.00170>
- 540 Toffanin, P., de Jong, R., Johnson, A., Martens, S., 2009. Using frequency tagging to
541 quantify attentional deployment in a visual divided attention task. *Int. J. Psychophysiol.*
542 72, 289–98.
- 543 Traub, R.D., Whittington, M.A., Buhl, E.H., Jefferys, J.G., Faulkner, H.J., 1999. On the
544 mechanism of the gamma --> beta frequency shift in neuronal oscillations induced in
545 rat hippocampal slices by tetanic stimulation. *J. Neurosci.* 19, 1088–105.
- 546 van Ede, F., de Lange, F., Jensen, O., Maris, E., 2011. Orienting Attention to an Upcoming
547 Tactile Event Involves a Spatially and Temporally Specific Modulation of Sensorimotor

- 548 Alpha- and Beta-Band Oscillations. *J. Neurosci.* 31, 2016–2024.
549 <https://doi.org/10.1523/JNEUROSCI.5630-10.2011>
- 550 Vanrullen, R., Busch, N.A., Drewes, J., Dubois, J., 2011. Ongoing EEG Phase as a Trial-by-
551 Trial Predictor of Perceptual and Attentional Variability. *Front. Psychol.* 2, 60.
552 <https://doi.org/10.3389/fpsyg.2011.00060>
- 553 Varela, F., Lachaux, J.-P., Rodriguez, E., Martinerie, J., 2001. The brainweb: Phase
554 synchronization and large-scale integration. *Nat. Rev. Neurosci.* 2, 229–239.
555 <https://doi.org/10.1038/35067550>
- 556 Vialatte, F.-B., Maurice, M., Dauwels, J., Cichocki, A., 2010. Steady-state visually evoked
557 potentials: focus on essential paradigms and future perspectives. *Prog. Neurobiol.* 90,
558 418–38. <https://doi.org/10.1016/j.pneurobio.2009.11.005>
- 559 Watson, A.B., Pelli, D.G., 1983. Quest: A Bayesian adaptive psychometric method. *Percept.*
560 *Psychophys.* 33, 113–120. <https://doi.org/10.3758/BF03202828>
- 561 Willenbockel, V., Sadr, J., Fiset, D., Horne, G.O., Gosselin, F., Tanaka, J.W., 2010.
562 Controlling low-level image properties: The SHINE toolbox. *Behav. Res. Methods* 42,
563 671–684. <https://doi.org/10.3758/BRM.42.3.671>
- 564 Williams, P.E., Mechler, F., Gordon, J., Shapley, R., Hawken, M.J., 2004. Entrainment to
565 video displays in primary visual cortex of macaque and humans. *J. Neurosci.* 24, 8278–
566 88. <https://doi.org/10.1523/JNEUROSCI.2716-04.2004>
- 567 Worden, M.S., Foxe, J.J., Wang, N., Simpson, G. V, 2000. Anticipatory biasing of
568 visuospatial attention indexed by retinotopically specific alpha-band
569 electroencephalography increases over occipital cortex. *J. Neurosci.* 20, RC63.
- 570

Normal trial (75%)



Catch trial (25%)

